J Mater Sci (2010) 45:1453–1458
DOI 10.1007/s10853-009-4100-9

Structural, thermal expansion and heat capacity study of lead-free $[(1 - x)(Na_{0.5}Bi_{0.5})–xBa]Zr_{1-y}Ti_yO_3$ ceramics

J. Suchanicz · G. Stopa · J. Kusz · M. Zubko · W. Hofmeister · M. Antonova · A. Kalvane · M. Dambekalne · A. Sternberg · I. Jankowska-Sumara · B. Garbarz-Glos · D. Wcisło · K. Konieczny · K. Pytel · A. Finder

Received: 21 July 2009 / Accepted: 30 November 2009 / Published online: 15 December 2009

Abstract Lead-free ceramics of $Na_{0.5}Bi_{0.5}TiO_3$–Ba(Ti,Zr)O_3 (NBT–BTZ) were prepared by solid phase hot pressing sintering process. The obtained samples show perovskite structure. Structural, the heat capacity, thermal expansion and pyroelectric measurements were made in wide temperature range. The broad anomalies of heat capacity and thermal expansion were observed, which approximately correspond to structural, pyroelectric and dielectric properties. It was concluded that these anomalies can be connected with temperature features of polar regions and with formation of long-range ferroelectric state. The obtained results are discussed in the framework of foreign ions/lattice imperfections, which create local electric and elastic fields. The NBT–BTZ system is expected to be a new promising candidate for lead-free electronic ceramics.

J. Suchanicz (✉) · G. Stopa · I. Jankowska-Sumara · B. Garbarz-Glos · D. Wcisło · K. Konieczny
Institute of Physics, Pedagogical University, ul. Podchorazych 2, 30-084 Krakow, Poland
e-mail: sfsuchan@ap.krakow.pl

J. Kusz · M. Zubko
Institute of Physics, University of Silesia, ul. Uniwersytecka 4, 40-007 Katowice, Poland

W. Hofmeister
Department of Gemstone Res, Johannes Gutenberg Universität Mainz, 55099 Mainz, Germany

M. Antonova · A. Kalvane · M. Dambekalne · A. Sternberg
Institute of Solid State Physics, University of Latvia, Kengaraga 8, 1063 Riga, Latvia

K. Pytel
Institute of Technics, Pedagogical University, ul. Podchorazych 2, 30-084 Krakow, Poland

A. Finder
High National School, ul. Mickiewicza 21, 38-500 Sanok, Poland

Introduction

Lead-based materials as PZT and PZT-based multicomponent ceramics are most widely used due to their excellent piezoelectric properties. However, the high volatilization of toxic PbO during sintering process not only causes environmental pollution, but also generate compositional inhomogeneities and formation of the unwanted pyrochlore phase. Moreover, there are problems with utilization of these materials. The use of lead-based piezoelectric materials may be prohibited in the near future. Therefore, much effort is being put into the search of lead-free materials with properties comparable with those found in lead-based ceramics. Some lead-free materials, including $Na_{0.5}Bi_{0.5}TiO_3$ (NBT) and NBT-based solid solutions yield excellent properties and could be good candidates for replacing materials based on lead [1–15].

NBT exhibits two structural phase transitions: first from ferroelectric rhombohedral to tetragonal phase (~260–350 °C) and the second one to paraelectric high temperature cubic phase (520–540 °C). A broad maximum of the electric permittivity (~320 °C) does not correspond to any phase transition and may originate from dielectric relaxation, which is suggested to be a response to electromechanical interaction between polar regions and the non-polar matrix [16]. The relaxor-like behaviour can be induced in NBT after adding Pb [17] or Ba [3, 18–25] ions. In order to future improving the properties of NBT-based materials, it is necessary to develop new NBT-based lead-free ceramics.

In this article, we obtained NBT-based ceramics by partial substitution of A-site ions $(Na_{0.5}Bi_{0.5})^{2+}$ by Ba^{2+} and B-site ions Ti^{4+} by Zr^{4+} of ABO_3 perovskite and their structural and heat properties were investigated. Recent study shows that these materials demonstrate diffuse phase transition and relaxor-like behaviour [26].

Experimental conditions

Sample preparation

Powders of $[(1-x)(Na_{0.5}Bi_{0.5})$–$xBa]Zr_{1-y}Ti_yO_3$, where $x = 0.06$, 0.085, 0.09, 0.1 and $y = 0.96$, 0.97 were obtained by solid phase synthesis from high purity grade oxides and carbonate: BaO, Na_2CO_3, Bi_2O_3, ZrO_2 and TiO_2. The mixture of starting raw materials were homogenized and milled in an agate ball mill in ethanol for 20 h, dried and then calcined. Due to multicomponent composition the two step calcination was chosen: the first one—4 h at 850 °C and the second one—2 h at 1,100 °C. Between the two calcinations the powder was homogenized and milled in ethanol environment in the ball mill. After the first calcination the powders contain 4–7% of pyrochlore phase, after the second one—single perovskite phase. The calcined powder were reground, cold pressed and sintered by hot pressing for 2 h at temperature ranging from 1,160 to 1,200 °C and pressure of 25 MPa, depending on BaO concentrations. The densities of the obtained samples are higher than 95% of the theoretical ones.

X-ray diffraction studies

For X-ray experiments a Seifert powder diffractometer (XRD 3000 TT) with a high temperature device from Materials Research Instruments (mir) was used. Measurements were made with CuKα radiation at 45 kV and 30 mA ($\lambda = 1.5405$ Å). The lattice parameters of compounds $[(1-x)(Na_{0.5}Bi_{0.5})$–$xBa]Zr_{1-y}Ti_yO_3$ (where $x =$ 0.06, 0.085, 0.09, 0.1 and $y = 0.$ 96, 0.97) has been characterized in the 2θ-range of 5–100° at room temperature. High temperature lattice parameters have been determined for four chosen compounds in the 2θ-range of 20–70° at 200, 450 and 700 °C in air. Lattice parameters were refined using the Full Prof Program [27].

Specific heat study

The specific heat measurements were made using a Netzsch DSC F3 Maia scanning calorimeter in the temperature range from −150 to 550 °C under argon atmosphere at a flow rate 30 mL/min. The specimen consisted of single piece of ceramics of the average mass 20 mg was placed in an alumina crucible. The data were collected on heating and cooling processes with constant rate of 10 °C/min.

Thermal expansion study

The thermal expansion measurements were made using a quartz displacement-capacitance transducer dilatometer with a sensitivity of 4×10^{-9} m. The data were collected on heating/cooling processes with constant rate of 1.5 °C/min.

Pyroelectric study

The pyroelectric currents were recorded by the use of Keithley 6517A meter by quasistatic method. Polarizing procedure proceeded in a *dc* electric field of 12 kV/cm applied at 250 °C and switched off at room temperature. Then the pyroelectric current were recorded at the heating rate 10 °C/min.

Dielectric study

Dielectric studies were carried out for silver electroded samples using an GW 821LCR meter within the temperature range 30–500 °C. The measuring electric field of strength ~ 20 V cm^{-1} and frequency from 100 Hz to 100 kHz was applied. The apparatus was set in capacity C and conductivity G mode. In order to reduce any ageing influence, prior to measurements the samples were annealed for 1 h at 550 °C. The data were collected regularly in steps of 0.1 °C on heating and cooling, with the temperature change at rate 120 °C/h, using an automatic temperature controller.

Results and discussion

For single crystals of $(1-x)$NBT–xBT ($x \leq 0.05$) besides main reflections satellite reflections were observed [13]. This is characteristic for many perovskites of this group [14, 15]. X-ray powder studies proved that our samples exhibit not only peaks from single phase of perovskite type, but also small additional peaks (Fig. 1). Detailed analysis showed that these peaks came rather from the existence of small amount of pyrochlore phase. It is not possible to refine local structure distortion from our X-ray powder pattern. However, broadening of diffraction peaks (FWHM) can be connected with crystal structure imperfections. Our studies showed that mean lattice parameter defined as a cube root of volume of the perovskite unit cell increases linear with the increase of Ba and Zr concentration (Fig. 2). This evolution agrees well with increasing value of the ionic radius of cations in the A-site and B-site

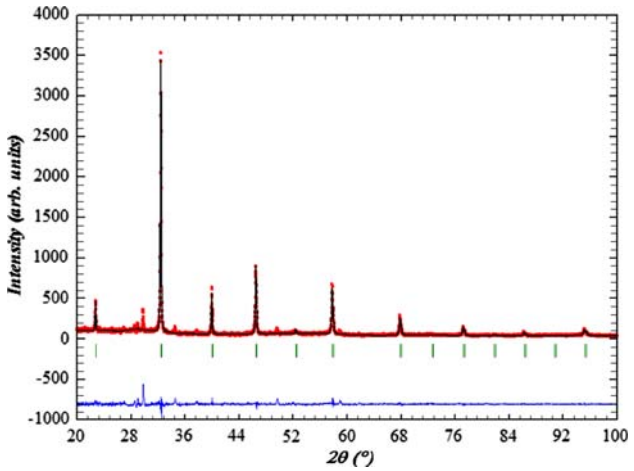

Fig. 1 X-ray powder diffraction pattern for the compounds $(Na_{0.5}Bi_{0.5})_{0.915}Ba_{0.085}Zr_{0.04}Ti_{0.96}O_3$. Besides main reflections (see *mark*), the additional reflections were observed

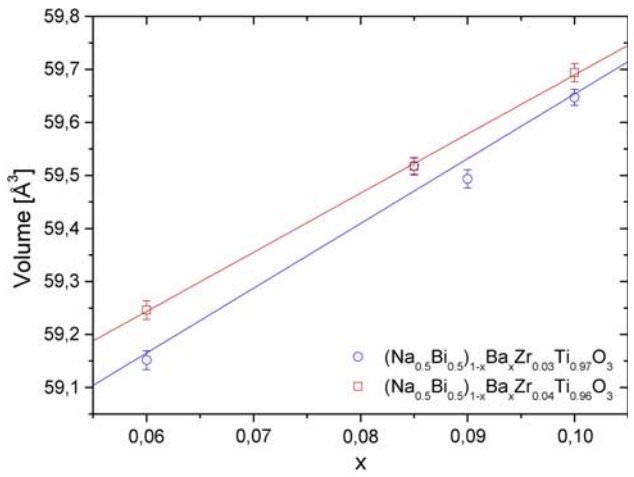

Fig. 2 Unit cell volumes for the NBT–BTZ ceramics (*x* describes content of Ba in the samples)

of the perovskite, since the radius of Ba^{2+} ion is greater than $(Na_{0.5}Bi_{0.5})^{2+}$ one and the radius of Zr^{4+} ion is greater than Ti^{4+} ion. Also the unit cell parameters increase linear with increasing of temperature (Fig. 3). The linear thermal expansion coefficients at 700 °C for lattice volume α_{Vol} are equal to $3.03(6) \times 10^{-5}$, $3.21(6) \times 10^{-5}$, $2.91(6) \times 10^{-5}$ and $2.93(6) \times 10^{-5}$ K^{-1} for $(Na_{0.5}Bi_{0.5})_{0.94}Ba_{0.06}Zr_{0.04}Ti_{0.96}O_3$, $(Na_{0.5}Bi_{0.5})_{0.94}Ba_{0.06}Zr_{0.03}Ti_{0.97}O_3$, $(Na_{0.5}Bi_{0.5})_{0.90}Ba_{0.10}Zr_{0.04}Ti_{0.96}O_3$ and $(Na_{0.5}Bi_{0.5})_{0.90}Ba_{0.10}Zr_{0.03}Ti_{0.97}O_3$, respectively.

The results of heat, pyroelectric and dielectric measurements for three samples: $(Na_{0.5}Bi_{0.5})_{0.94}Ba_{0.06}Zr_{0.04}Ti_{0.96}O_3$ (NBTB6Z4), $(Na_{0.5}Bi_{0.5})_{0.915}Ba_{0.085}Zr_{0.04}Ti_{0.96}O_3$ (NBTB8.5Z4) and $Na_{0.5}Bi_{0.5})_{0.90}Ba_{0.1}Zr_{0.04}Ti_{0.96}O_3$ (NBTB10Z4) have been shown (Figs. 4, 5, 6, 7, 8).

Figure 4 shows the temperature dependencies of heat capacity (C_p) for NBT–BTZ ceramics. As it can be seen,

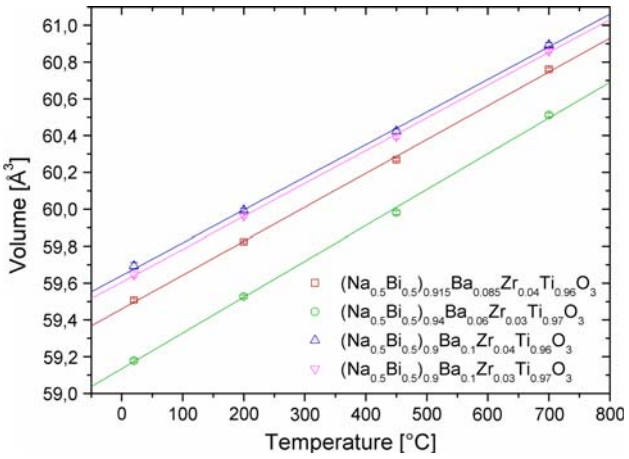

Fig. 3 Temperature dependence of the lattice volume of NBT–BTZ ceramics

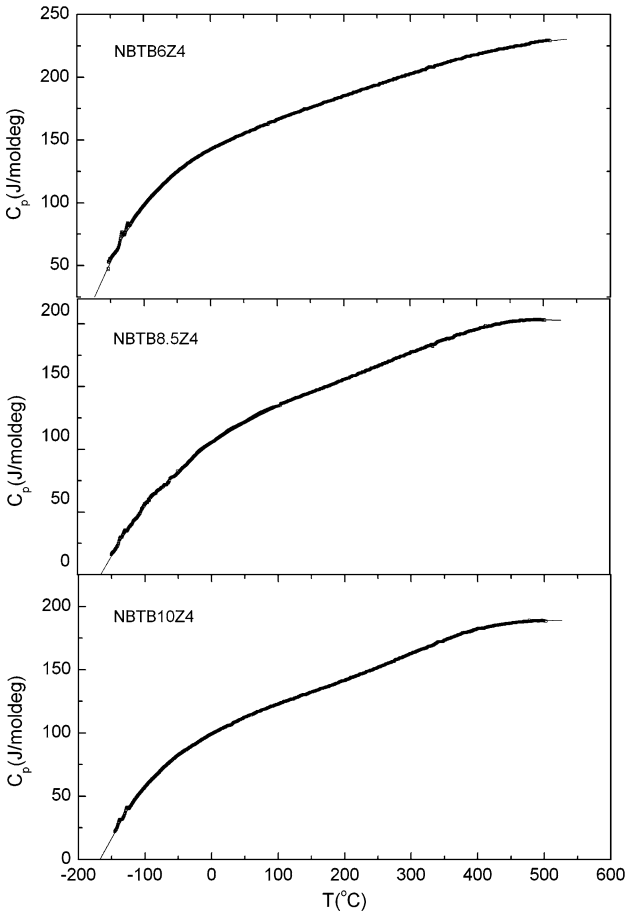

Fig. 4 Temperature dependence of the heat capacity of NBT–BTZ ceramics. The *solid line* is regular background contribution to the heat capacity

$C_p(T)$ curves do not exhibit clearly manifested anomalies typical for classical phase transitions. However, some broad blurry anomalies are visible (see also Fig. 5). Regular background contribution to the heat capacity have

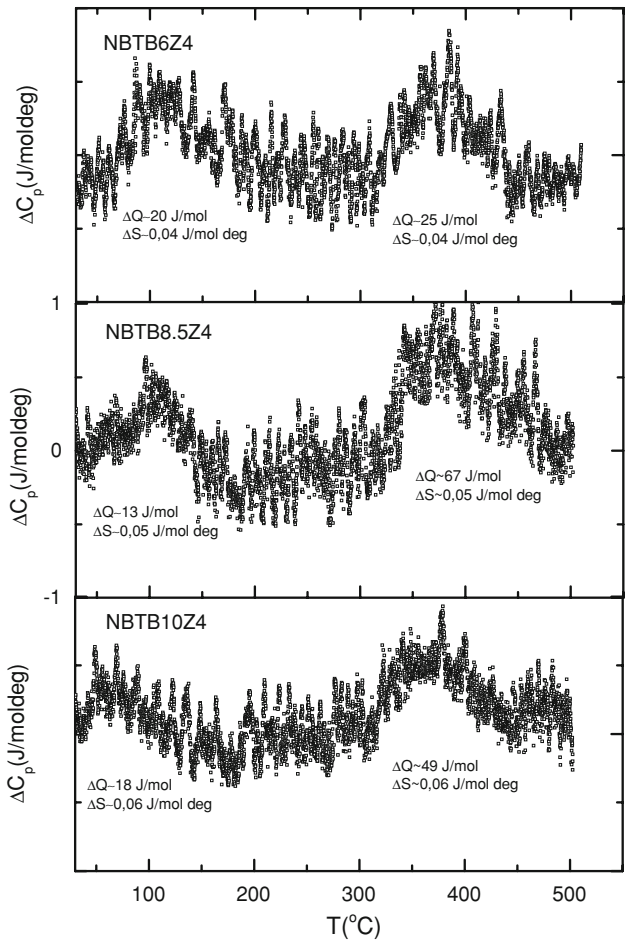

Fig. 5 Temperature dependence of the heat capacity excess of NBT–BTZ ceramics. For each anomaly, the approximately magnitude of heat effect ΔQ and entropy change ΔS are indicated. The units in *top* and *bottom panels* are the same as for *central panel*

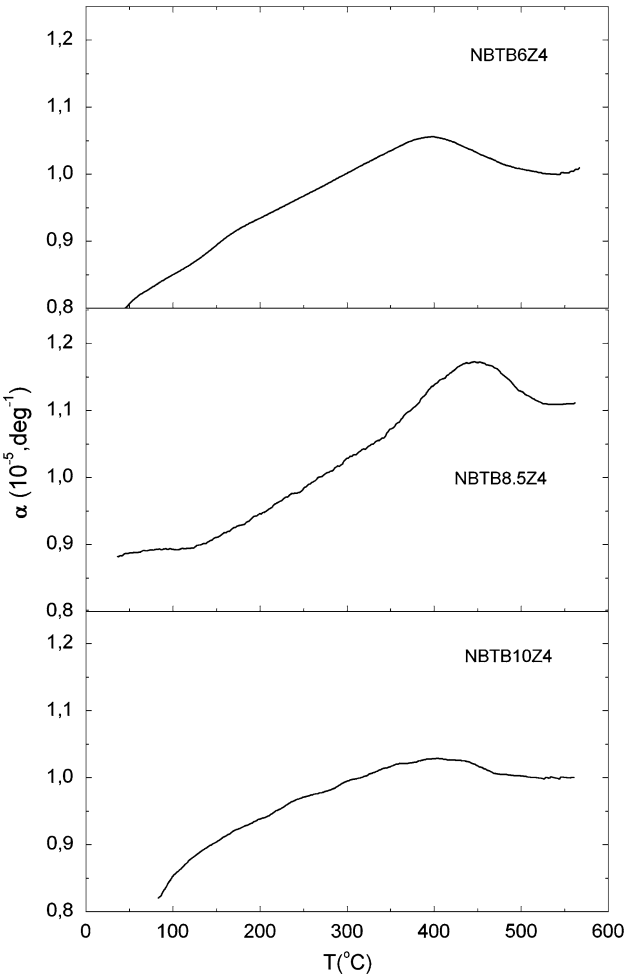

Fig. 6 Temperature dependence of the linear thermal expansion coefficient of NBT–BTZ ceramics

been estimated by fitting a polynomial function of temperature to the data. After subtracting the background thus determined, the excess heat capacity ΔC_p are obtained and shown in Fig. 5. The heat capacity anomalies ΔC_p reach only $13 \div 67$ J mol^{-1}. However, $\Delta C_p(T)$ dependencies distinguish some temperature ranges: ~90–180 °C and 320–470 °C for NBTB6Z4, ~80–180 °C and 250–470 °C for NBTB8.5Z4 and ~70–160 °C and 320–430 °C for NBTB10Z4. The entropy change associated with the anomalous behaviour of the heat capacity determined as $\Delta S = \int(\Delta C_p/T)\mathrm{d}T$ is small for all samples [$\sim(4-6)\times 10^{-2})R$, where R is the gas constant, Fig. 5], and is typical for displacive diffuse phase transformation.

Figure 6 shows the temperature dependencies of linear coefficient of thermal expansion (α) for NBT–BTZ ceramics. There are pronounced anomalies of α(T) at about 125 °C (small local minimum for NBTB6Z4 and NBTB8.5Z4, and change in the slope below this temperature for NBTB10Z4). Then α increases with increasing temperature up to about 380–430 °C, where broad anomaly exist.

Figure 7 shows temperature dependencies of pyroelectric current (i_p) for NBT–BTZ ceramics. As it can be seen, $i_p(T)$ dependencies show smeared anomalies at approximately the same temperature ranges as heat capacity and thermal expansion coefficient.

Figure 8 shows the temperature dependencies of electric permittivity (ε) for NBT–BTZ ceramics. As it can be seen, $\varepsilon(T)$ curves show anomalies in temperature range, which approximately corresponds to the same temperature range as heat capacity, thermal expansion and pyroelectric current (Figs. 5, 6, 7 for comparison).

The obtained results from the present study are characteristic for that observed in complex compounds or solid solutions, in which foreign ions occupy crystallographically equivalent lattice sites. The break of translational invariance caused by foreign ions/lattice imperfections leads to extreme broadening of the transition anomalies in these materials (so called *diffuse phase transition*). In some

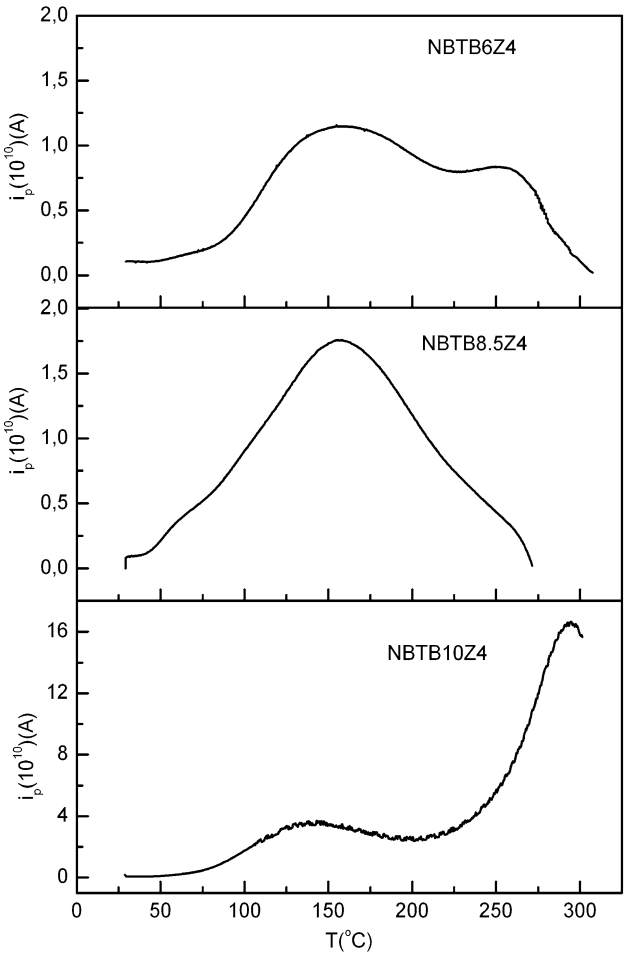

Fig. 7 Temperature dependence of the pyroelectric current of NBT–BTZ ceramics

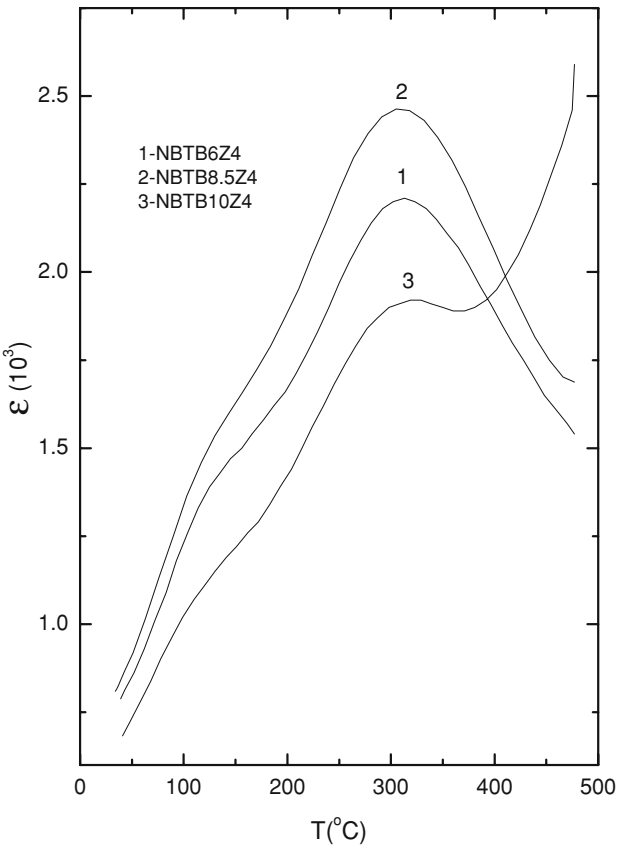

Fig. 8 Temperature dependence of electric permittivity of NBT–BTZ ceramics

group of these materials, the temperature T_m, at which ε reaches maximum and the height of ε maximum (ε_m) plotted as a function of temperature depends on the frequency. T_m shifts to higher temperatures and ε_m decreases when the frequency increases. Moreover, the random mean square polarization persists at temperatures several hundred centigrade above electric permittivity anomaly (polar nanoregions in nonpolar matrix exist). These materials are so called *relaxor ferroelectrics*.

The substitution of A-site ions $(Na_{0.5}Bi_{0.5})^{2+}$ by Ba^{2+} introduces additional disorder in this site. As this substitution is not isovalent, some charge imbalance in $Na_{0.5}Bi_{0.5}TiO_3$ can be created. Cation vacancies can be formed probably to compensate this charge imbalance, and random electric fields are thus expected. As the Ba^{2+} ion size is larger than that of $(Na_{0.5}Bi_{0.5})^{2+}$ ions, it may cause internal tensile stresses and random elastic fields are thus expected. It should be pointed out that Zr^{4+} substitution in B-site is isovalent, and does not affect drastically the charge state of $Na_{0.5}Bi_{0.5}TiO_3$. However, the Zr^{4+} ion size is larger than that of Ti^{4+} ions, and the random elastic fields are also expected from this substitution. These electric and elastic fields, which promote formation of polar regions, are very likely to be responsible for relaxor-like behaviour of NBT–BTZ system, as it was suggested in article [26].

Hysteresis loops measurements carried out for our samples show that ferroelectric state exists in the temperature range below local anomaly of $\alpha(T)$, $\varepsilon(T)$ and $i_p(T)$. Therefore, the low-temperature anomaly of C_p, which coincides with the anomaly of linear coefficient of thermal expansion, electric permittivity and pyroelectric current is connected with the formation of long-range ferroelectric state. However, high-temperature anomaly of C_p, which approximately coincides with main anomaly of electric permittivity is connected with temperature evolution of above-mentioned polar regions. Deviation from Curie–Weiss law, which appears in investigated samples from about 420 to 450 °C, confirms this supposition. These polar regions grown with decreasing temperature, start to interact (in the temperature region where main anomaly of ε and high-temperature anomaly of C_p exist), and then they become the nuclei of the emerging ferroeleectric phase.

Conclusions

The good quality ceramics of $[(1 - x)(Na_{0.5}Bi_{0.5})–xBa]Zr_{1-y}Ti_yO_3$ ($x = 0.06, 0.085, 0.09, 0.1$ and $y = 0.96, 0.97$) lead-free solid solutions were obtained by solid state hot pressing method.

X-ray tests showed that these ceramics consist of a single perovskite phase with small amounts of pyrochlore phase. The replacement of the $(Na,Bi)^{2+}$ ions by Ba^{2+} and Zr^{4+} ion by Ti^{4+} ion causes the increase of the mean lattice parameter of the pseudoperovskite unit cell. The prepared samples exhibit the features of diffuse phase transition and ferroelectric relaxor. We can conclude that these behaviour of NBT–BTZ solid solutions can be connected with crystal structure imperfections due to foreign ions substitution, which promote formation of polar regions. It was concluded, that the observed anomalous behaviour of thermal properties is connected with temperature dependence of dynamic and sizes of polar regions and with formation of macroscopic ferroelectric phase. It is obvious that the obtained ceramics are promising materials for high-frequency electromechanical transducer application.

References

1. Elkechai O, Manier M, Mercurio IP (1996) Phys Stat Sol (a) 157:499
2. Elkechai O, Marchet P, Thomas P, Manier M, Mercurio IP (1997) J Mater Chem 7:91
3. Chiang YM, Farrey GW, Soukhojak AN (1998) Appl Phys Lett 73:3683
4. Suchanicz J, Mercurio IP, Marchet P, Kruzina TV (2001) Phys Stat Sol (b) 225:459
5. Suchanicz J, Kusz J, Bohm H, Stopa G (2007) J Mater Sci 42:7827. doi:10.1007/s10853-007-1635-5
6. Suchanicz J, Mercurio JP, Konieczny K (2002) Ferroelectrics 268:357
7. Said S, Mercurio JP (2001) J Eur Ceram Soc 21:1333
8. Takenaka T, Maruyama K, Sakata K (1991) Jpn J Appl Phys 30:2236
9. Yu Z, Guo R, Bhalla AS (2000) Appl Phys Lett 77:1535
10. Farhi R, Marssi ME, Simon A, Ravez J (1999) Eur Phys J B 9: 599
11. Liou JW, Chiou BS (2000) J Mater Sci 11:637. doi:10.1023/A:1008945200078
12. Ravez J, Simon A (2000) Phys Stat Sol (a) 178:793
13. Suchanicz J, Glos B, Stopa G, Kruzina T, Kusz J, Zubko M, Hofmeister W, Jankowska-Sumara I, Wcislo D, Konieczny K, Rosiek R, Finder A, Pytel K, Dambekalne M, Sternberg A (2009) Integr Ferroelectr 108:98
14. Zvigzds JA, Kapostins PP, Zvirgzde JV, Kruzina TV (1982) Ferroelectrics 40:75
15. Kusz J, Suchanicz J, Böhm H, Warczewski J (1999) Phase Transit 70:223
16. Suchanicz J (1998) Ferroelectrics 209:561
17. Suchanicz J, Mercurio JP, Said S, Garbarz-Glos B (2002) Phys Stat Sol (a) 193:179
18. Chu B-J, Li G-R, Jiang X-P, Chen D-R (2000) J Inorg Mater 15:815 (in Chinese)
19. Chu B-J, Li G-R, Yin Q-R, Zhang W-Z, Chen D-R (2001) Acta Phys Sin 50:2012 (in Chinese)
20. Suchanicz J, Kusz J, Böhm H, Duda H, Mercurio JP, Konieczny K (2003) J Eur Ceram Soc 23:1559
21. Kimura T, Takahashi T, Saito Y (2004) Ceram Int 30:1161
22. Ranjan R, Dviwedi A (2005) Solid State Commun 135:394
23. Chu BJ, Chen DR, Li GR, Yin QR (2002) J Eur Ceram Soc 22:2115
24. Suchanicz J, Kusz J, Böhm H (2003) Mater Sci Eng B 97:154
25. Gomah-Pettry IR, Said S, Marchet P, Mercurio JP (2004) J Eur Ceram Soc 24:1165
26. Suchanicz J, Stopa G, Antonova M, Kalvane A, Dambekalne M, Sternberg A, Jankowska-Sumara I, Smiga W, Glos T, Wcisło D, Konieczny K (2009) Integr Ferroelectr 102:62
27. Rodriguez-Carvajal J (1993) Physica B 55:129